

# APPLICATION OF HARMONIC BALANCE METHOD TO THE SIMULATION OF UNSTEADY ROTOR/STATOR INTERACTION IN THE SINGLE STAGE

*Grigoriev A.V.<sup>1</sup>, Iakunin A.I.<sup>1</sup>, Kuznechov N.B.<sup>1</sup>, Kondratiev V.F.<sup>2</sup>, Kortikov N.N.<sup>2</sup>*

(1) – JSC ‘Klimov’, St - Petersburg, Russia  
e-mail: iak1961@rambler.ru

(2) – Turbomachinery Department, Theoretical Foundations of Thermotechnics Department,  
St - Petersburg State Polytechnical University, Russia  
e-mail: [n-kortikov@yandex.ru](mailto:n-kortikov@yandex.ru)

## ABSTRACT

The harmonic balance method which is included in STAR CCM+ code can simulate the whole unsteady flow at considerably reduced CPU costs. This paper represents 3D flow in turbine cascade in which the harmonic balance method is applied for modeling rotor – stator interaction and pressure fluctuations near trailing edges. Computational results are compared with experimental results which show importance of unsteady effects.

## NOMENCLATURE

$B_1$	number airfoils in stator row
$B_2$	number airfoils in rotor row
CFD	Computational Fluid Dynamics
$c$	chord
$g$	pitch
$d$	diameter
$M$	number modes
$N$	nodal diameter
$m_1, m_2$	integer values for nodal diameter
$n_1, n_2$	integer values for harmonic balance frequencies
$\vec{r} = \vec{r}(X, Y, Z)$	coordinates vector
$V$	velocity magnitude
LPI	Leningrad Polytechnic Institute (now Saint - Petersburg State Polytechnical University)
Real	real part of solution
Imag	imaginary part of solution
$\alpha_1$	inlet vane angle
$\beta_1, \beta_2$	inlet and exit blade angle
$\tau$	time
$\omega$	harmonic balance frequency
$\Omega$	angular velocity
0	zero - th mode
1	stator
2	rotor

## INTRODUCTION

High cycle fatigue is due to the flow unsteadiness that originates in the relative motion between rotor and stator airfoils. The understanding of pressure and velocity fluctuations associated with

blade row interactions is fundamental to improve both the aerodynamic performance and mechanical integrity of future generations of aero-engines (Breugelmans, 2005).

3D CFD simulation of turbine blade rows is central to the aerodynamic development of advanced turbines. With the advancement in computational methods, models and flow solvers and the general availability of powerful computing facilities, blade row simulation has evolved from steady single passage simulation, to steady multiple blade row simulation to unsteady single and multiple blade row simulation.

Steady single blade row solution is now very fast, but information on adjacent rows must be specified, and the ability for adjacent rows to interact is only explicit at best. Steady multiple blade row methods such as the “mixing plane” approach and its variants extend simulation realism by including adjacent blade row effects, albeit in a limited manner. The limitation is due to the circumferential averaging and the manner in which information is communicated across the interface from one row to the next. Despite such limitations, multi-blade row “**stage**” or “**mixing-plane**” methods represent a reasonable compromise between accuracy and efficiency and hence remain valuable and powerful tools for the designer/analyst (Biesinger et al. 2010).

Since turbines are already very efficient, it seems that further improvement to efficiency and durability requires a better understanding of observed physical phenomena such as wake propagation, wake-blade interaction, convection of hot streaks, transient loading variation, laminar-turbulent transition, complex endwall flows and primary-leakage flow interactions. The designer may wish to use a variety of tactics to improve the design, such as changing the loading distribution, **blade “clocking”**, adjusting sweep and lean or endwall contouring. The effect of each adjustment must be understood in the context of how it interacts with the unsteady flow, or not.

In **Transient Rotor-Stator (TRS)** simulations the true change in relative position of the rotor and stator are accounted for in fully implicit interface discretization. In these simulations, either full wheel is assumed or the smallest possible circumferential sector with an integer number of blades, according to the pitch ratio, is modeled with standard periodicity applied to the blade ensemble (unity ensemble pitch ratio between rotor and stator rows).

Transient calculations are performed using a recently-developed family of transient blade row methods known as “transformation methods”, namely Profile Transformation, Time Transformation and Fourier Transformation (Connell et al, 2011).

In the **Profile Transformation (PT)** method a scaling procedure is applied automatically to solution profiles as part of the TRS implementation, when ever the rotor-stator pitch ratio is not unity. In this approximate method, single blade passages per row with different pitch lengths can be modeled without the need to geometrically scale or modify the blade geometry. Regular periodicity is imposed for each passage and flow profiles across rotor/stator interfaces are automatically stretched or compressed as needed according to the pitch ratio while maintaining full conservation.

The **Time Transformation (TT)** method can be considered as a correction to the Profile Transformation method in that the flow equations are transformed in time to ensure that the pitch wise boundaries are truly periodic. Therefore, the Time Transformation method maintains the robustness of the solution and also accounts for the correct blade passing signals between the rotor and stator.

In **Fourier Transformation (FT)** method the flow history on the phase-shifted pitchwise boundaries are stored using Fourier series at the blade passing frequency and its higher harmonics. At the rotor-stator interface flow information is stored using double- Fourier series by decomposing the solution history in time and azimuthal direction. The solution is then reconstructed on each side of the interface using Fourier coefficients from the opposite side. Most importantly this method can be extended to handle multi-disturbance problems and thus multi - stage turbomachinery configurations.

**Harmonic Balance (HB)** techniques have been developed that can include dynamic nonlinear effects and at the same time can reduce time for solution (He et al, 1998 and Hall et al, 2002). In this approach, the unsteady flow is assumed to be temporally and spatially periodic, as in

a turbomachinery flow. The flow variables are represented by a Fourier series in time with frequencies that are integer multiples of the original excitation frequency (He et al, 2006 and Vilmin et al, 2009). The dependent variables are the coefficients of the Fourier series for each conservation variables. The Fourier series are then inserted into the unsteady fluid dynamics equations, and the resulting expressions are balanced by collecting terms with same frequency. This results in a set of coupled complex partial differential equations, one for each frequency retained in the model. The method, which was later improved by storing the dependent variables at a number of sub-time levels over one period, has been applied to many configurations (Weiss et al, 2011 and Custer et al, 2012).

The focus of this paper is Harmonic Balance transient CFD method which is characterized fast solution to time periodic flow, simultaneous coupled solution on several time instances, solve like steady - state flow simulations, uses harmonics to reconstruct solution, apply phase-shifted boundary conditions and resolve pitch – change. All calculations are performed with a pre-release version of STAR CCM+ 7.04.006.

## PHYSICAL MODELLING

Physical modeling of transient phenomena in the turbine stage was conducted on experimental turbine ETN - 4 LPI with pressurized air (Kondratiev, 1977). When you create the experimental test facility, special attention was paid to ensuring uniform around the circumference of the air supply with low turbulence. Pulsating flow in a circle in front diffuser is 1%, and the degree of turbulence - 1.5%. Turbine flow passage is provided with a constant height of the channel in the meridian plane. The average diameter of the impeller -430mm at a height blades -70mm. Number of vanes – 24, number of blades – 48 (Figure 1). Geometric characteristics of the gratings are presented in Table 1.

**Table 1 – Two rows parameters**

Section	d m	g <sub>1</sub> m	g <sub>2</sub> m	c <sub>1</sub> m	c <sub>2</sub> m <sub>2</sub>	α <sub>1</sub> degrees	β <sub>1</sub> degree s	β <sub>2</sub> degrees
Bottom	0.36	0.0471	0.0269	0.078	0.035	25°10'	34°16'	36°30'
Mid - span	0.43	0.0562	0.0322	0.078	0.037	26°20'	58°25'	34°32'
Top	0.50	0.0654	0.0374	0.078	0.043	28°20'	94°50'	30°16'

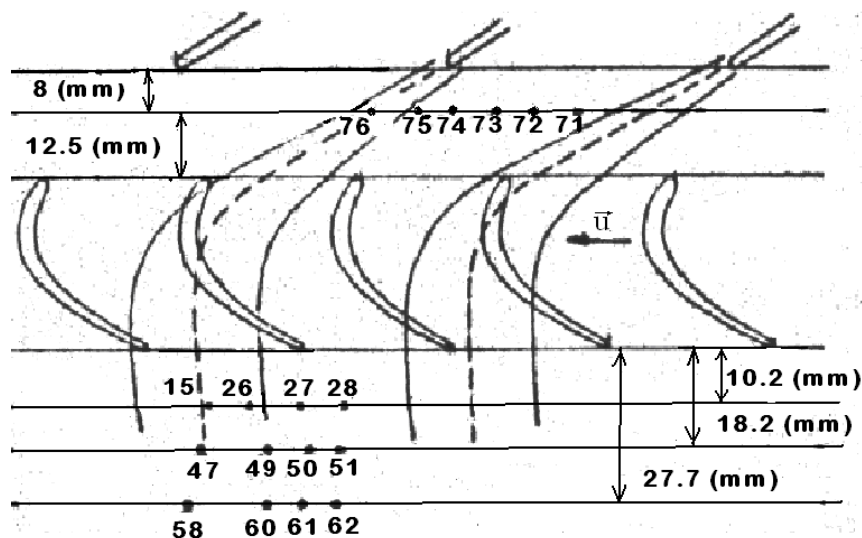


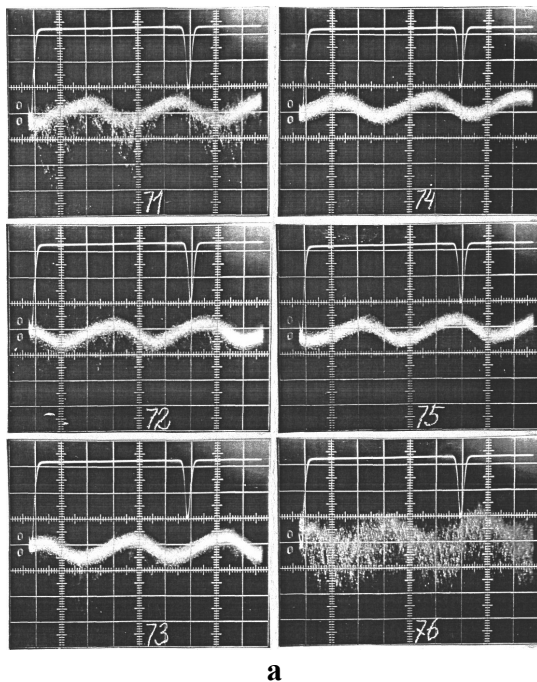
**Figure 1 – Flow scheme in the ETN - 4 LPI turbine stage**

In turbomachinery the Strouhal number  $St_2 = (fg_2/V_2)$ , where  $f$  is the blade passing frequency. In our case  $St_2 = 0.772$ , exit Reynolds number  $Re_2 = 3.7 \cdot 10^5$ , exit Max number  $M_2 = 0.464$ .

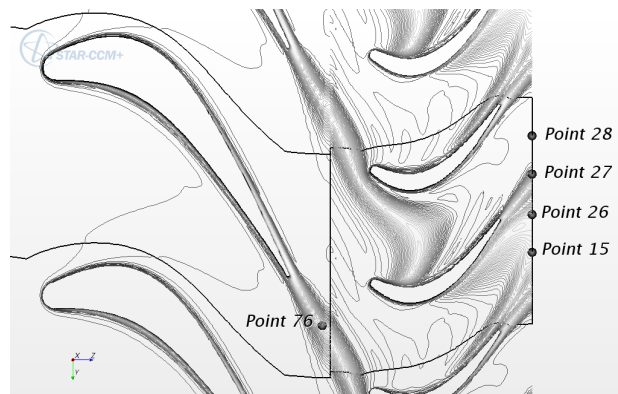
The flow in the turbine is periodically unsteady, so we must check the instantaneous velocity. The single channel thermo-anemometer was applied to variable measurement in time of velocity with a constant temperature of a wire. The probe of the thermo-anemometer had one wire focused radially, with a delay with a diameter of 5 microns and 2 mm long. The thermo-anemometer provides measurement of velocity pulsations in the range of frequencies from 0 Hz to 40 kHz.

Repeated calibrating of a probe and the analysis of defining factors showed that instrument errors don't exceed 0.1%. Experiment of use of the thermo-anemometer in flowing part of the turbine showed importance of the accounting of the error connected with honors of temperature from temperature at performance of calibrating. The corresponding possible error was excluded by means of the special correcting amendment to the equation of the thermo-anemometer, temperature considering this difference. This type of an error is estimated of 3%.

Waveform records by an electron oscilloscope, which is connected to the output of hot-wire anemometer. Fig. 2a shows the waveform of the instantaneous velocity in axial gap of turbine. At the top of the waveform recorded signal timer position blades.



a



b

**Figure 2 – Experimental data for velocity in axial gap of turbine (a); CFD monitor points (b)**

To measure the time-varying pressure on the blade surface pressure sensor is used as a flexible plate is rigidly clamped in the housing on the perimeter. The plate is deformed under the influence of the measured variable pressure, and these strain gage by flintlock converted to an electrical signal.

As shown in Fig. 2b, edge wakes vanes create disturbances that come out of interscapular channels in the form of areas of increased c turbulent viscosity. At the exit of the impeller stationary probe anemometer records the velocity fluctuations (Figure 3) generated by: 1) an uneven potential field of blades, 2) edge wakes of blades, and 3) the velocity perturbations that are generated periodically at the entrance to each moving channel and pass through it, appropriately transformed.

The nature of the velocity fluctuations in the set point of the next depends on the story, which is determined by the nature of the flow near the concave and convex surface of the blade, as well as the trailing edge. As can be seen from the waveforms (Figure 3), the left slope of the pulse is

formed regular pulsations, which indicates a stable and steady airflow around the convex surface. The intensity of the turbulent fluctuations can be seen in scale random components on the waveform. In Fig. 3 shows that the level of turbulent velocity fluctuations in the turbulent region decreases with distance from the trailing edge of the grid.

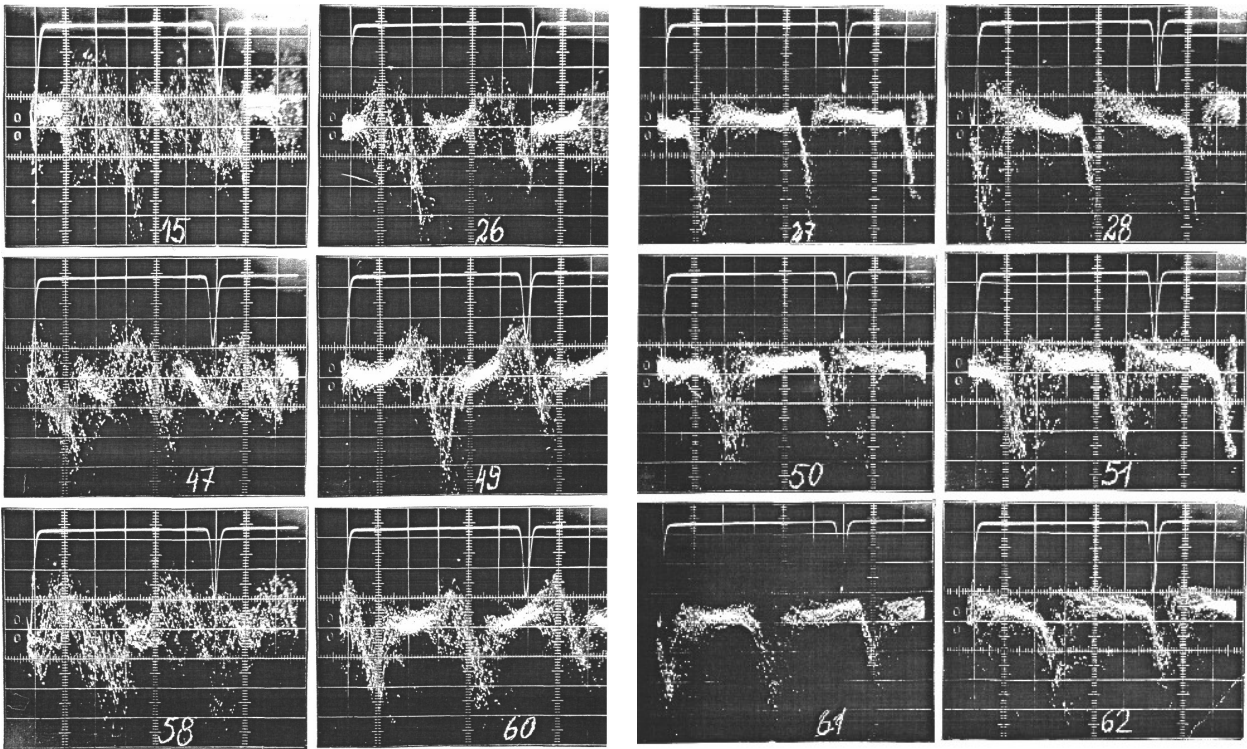


**Figure 3 - Experimental data for velocity behind the rotor**

The high level of random fluctuations in the components of the right slope of the pulse shows the high turbulence of the flow around a concave surface of the blade. Turbulence is the action destabilizing influence of Coriolis forces acting on the particles of the fluid with a radial velocity component. Under the action of Coriolis forces the fluid particles move in the direction of the concave surface of the blade, which is accompanied by turbulization boundary layer. On the convex surface | Coriolis forces pressed flow to the blade, so here the flow is stable

## COMPUTATIONAL METHOD

The unsteady flow field in a turbomachine blade passage is governed by the Navier - Stokes equations, written in integral form for a rigid, arbitrary control volume in a relative frame of reference rotating steadily with angular velocity  $\Omega$ :

Since the solution function  $W$  is periodic in time, it can be represented by the Fourier series:

$$W(\vec{r}, \tau) = \sum_{m = -M}^M W_m(\vec{r}) \exp(i\omega m \tau), \quad (1)$$

where  $\omega$  is the fundamental frequency of the disturbance,  $M$  is the number of harmonics retained in the solution, and  $W_m$  are the Fourier coefficients.

The frequencies and wavelengths of disturbances within the rows of a multistage machine are determined by the blade counts in the individual blade rows and the rotation rate of the rotor. Disturbances in the two rows with respective blade counts  $B_1, B_2$  will have circumferential waves

numbers (nodal diameters) equal to  $N = m_1 B_1 + m_2 B_2$ , where  $m_1$  and  $m_2$  can take on all integer values. The frequency in the stationary frame of reference is given by  $\omega = n_2 B_2 \Omega$ . In the rotor frame of reference, the frequencies is given by  $\omega = -n_1 B_1 \Omega$ .

The harmonic balance equations are discretized by means of a cell - centered, polyhedral-based, finite-volume scheme having second order spatial accuracy. The convective fluxes are evaluated by a standard upwind, flux-difference splitting and the diffusive fluxes by a second-order central difference.

A pseudo-time derivative is introduced into the discretized equations to facilitate solution of the steady, harmonic balance equations by means of a time marching procedure. An Euler implicit discretization in pseudo-time is applied to yield a coupled, linear system containing equations from all time levels linked at every point in the domain by the pseudo-spectral operator. Approximate factorization is employed to effectively decouple the time levels, and an algebraicmultigrid (AMG) method is used to solve the linear system associated with each time level.

Complex periodicity conditions are applied at the periodic boundaries in the rotational direction to reduce the computational domain to a single passage in each row. Non-reflecting, far field boundary conditions are applied at the inflow and outflow boundaries of the domain to prevent spurious unsteady numerical disturbances from reflecting back into the computational domain. This permits the use of truncated computational domains, with boundaries positioned near to the leading and trailing edges of the outermost blade rows. In the far field, the solution may be thought of as comprised of upstream and downstream moving waves. At each radial station along the far field, we apply two dimensional nonreflecting boundary conditions.

For the zero nodal diameter steady modes, traditional steady inflow or outflow boundary conditions are applied. Total pressure, total temperature, and flow angle of the mean flow are specified at the inflow boundary, and the static pressure of the mean flow is specified at the outflow boundary. Finally, having modified the far field spinning modes, the mode coefficients are inverse Fourier transformed in space and time to obtain the time level solutions along the far field boundary

## COMPUTATIONAL RESULTS

The harmonic balance method requires only a single blade passage be meshed. A structured HOH mesh is generated for each of the two blade rows, as shown in Figure 4. The inlet and exit grid planes for each of the blade rows correspond to the axial planes where test data is available. The blade passage mesh is made up of 1.3 million cells with a near wall spacing of  $y^+ = 1.0 - 16$ .

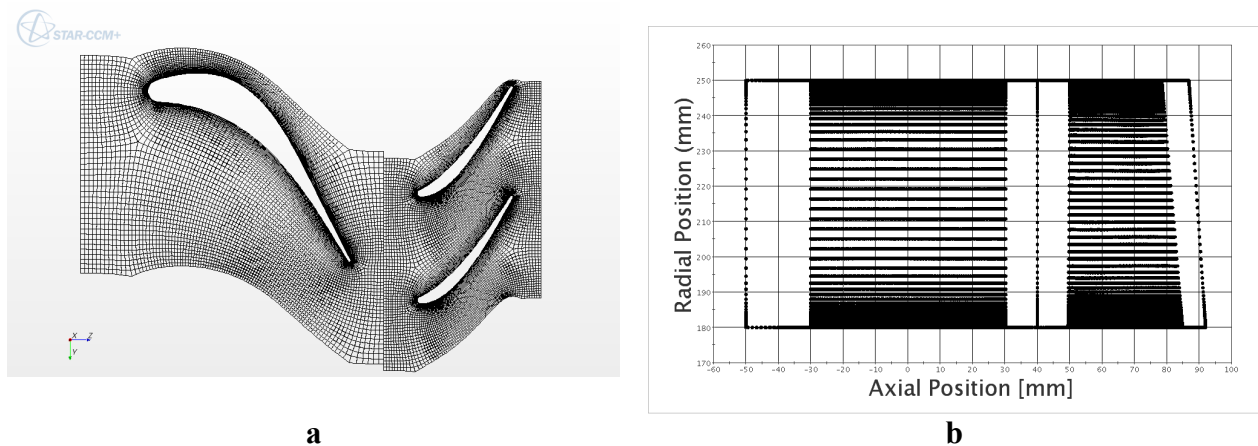


**Figure 4 - Computational mesh for HB and TRS methods (a); meridional plane of passages in the stage (b)**

The test conditions for the case correspond to an inlet reference total pressure of about 0,14 MPa and an exit gauge pressure of about 0,0 Pa. Angular velocity is equal 5000 rpm. Total temperature - 350 K. With the Harmonic Balance method non - reflecting treatment is enabled on the inlet and exit as well as the inter - row interfaces.

To provide a good initial condition to the HB solver, grid sequencing initialization is used. This procedure solves the steady Navier - Stokes equations and mixing plane approach on progressively finer grids. Once the initial condition is obtained, the HB solver is invoked and simply run to convergence.

The HB solver models the fluid as an ideal gas with turbulence closure provided by the Spalart - Allmaras turbulence model. The solver is run with a CFL number of 5.0, and separate trials are conducted retaining one, three, and five modes. The solver has converged to a periodic, unsteady solution within 4000 - 5000 iterations (Figure 5a). The TRS solver uses a time step is equal  $510^{-5}$ s. This value correspond 5 steps per vane passing (10 inner iterations per time step). Calculation results on Figure 5b show stable periodic behavior of velocity for three monitor points within 47000 inner iterations.

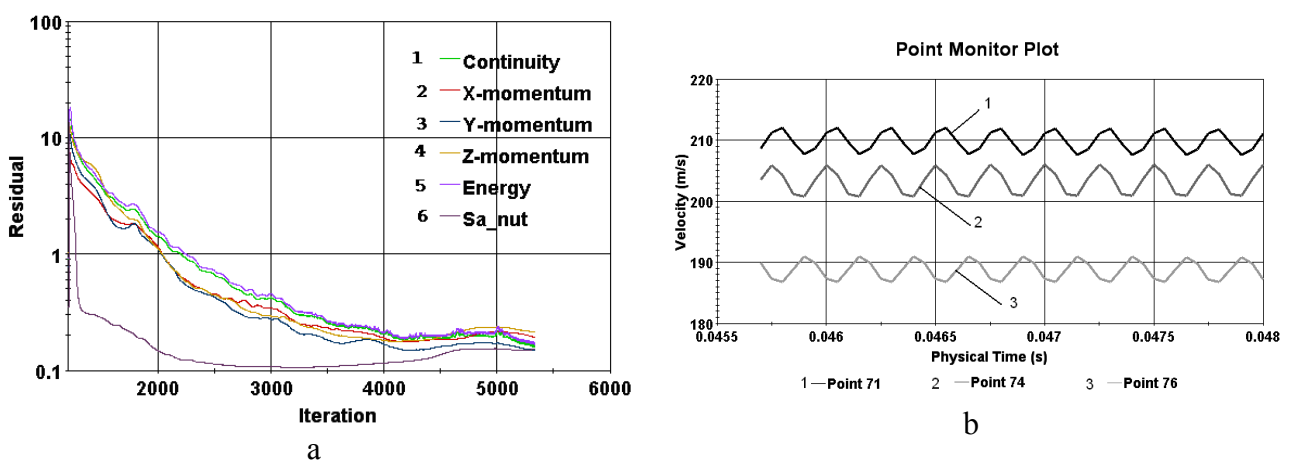


**Figure 5 – Harmonic balance solution residuals for a five mode trial (a); periodic behavior of velocity - TRS solver model (b)**

Assessment of the effectiveness of the two methods of calculation is carried out on the basis of the comparison of time required for obtaining of non-stationary periodic solutions on the interval of time, sufficient for the passage of at least one rotation of the impeller.

The HB-results showed that CPU time is increased in 7 times for 5 modes compared time when calculating with one mode. Using 3 modes CPU time is increased (for one iteration) in 3.3 times in comparison with one-mode approximation. The acceleration of the calculation, which is defined as the ratio of the CPU time required to obtain a periodic solution using the TRS method to the CPU time of the decision on the HB method is 1:2 - five modes, 1:1 - three modes and 3:1 - one mode. Hence, the substantial savings (three times) is observed only in the case of one - mode approximation.

It is important to note that in all cases the calculations were carried out at the same calculation grid, including two blades (figure 4a). This suggests the possible reduction of the computational expenditures also for the three modes using the harmonic balance method on the grid that contains only one межлопаточный channel impeller.

Figures 6a, c present instantaneous predictions of turbulent viscosity at mid - span for the HB and TRS solutions. The stator wake enters the rotor passage and grows both laterally and in the stream wise direction. This process continues as the stator wake is “chopped” by the leading edge of the rotor blade and convects downstream.

Figure 6b shows the velocity magnitude change on the interface line between two rows. Velocity profile has two minima, one of them (with great shame) corresponds to edge wakes of the vane and the second minimum is associated with upstream acting of blade leading edge on flow in axial gap.

Velocity profile on Figure 6d (along line CD on Fig. 6c)) also is characterized two minima which are associated with edge wakes of two blades.

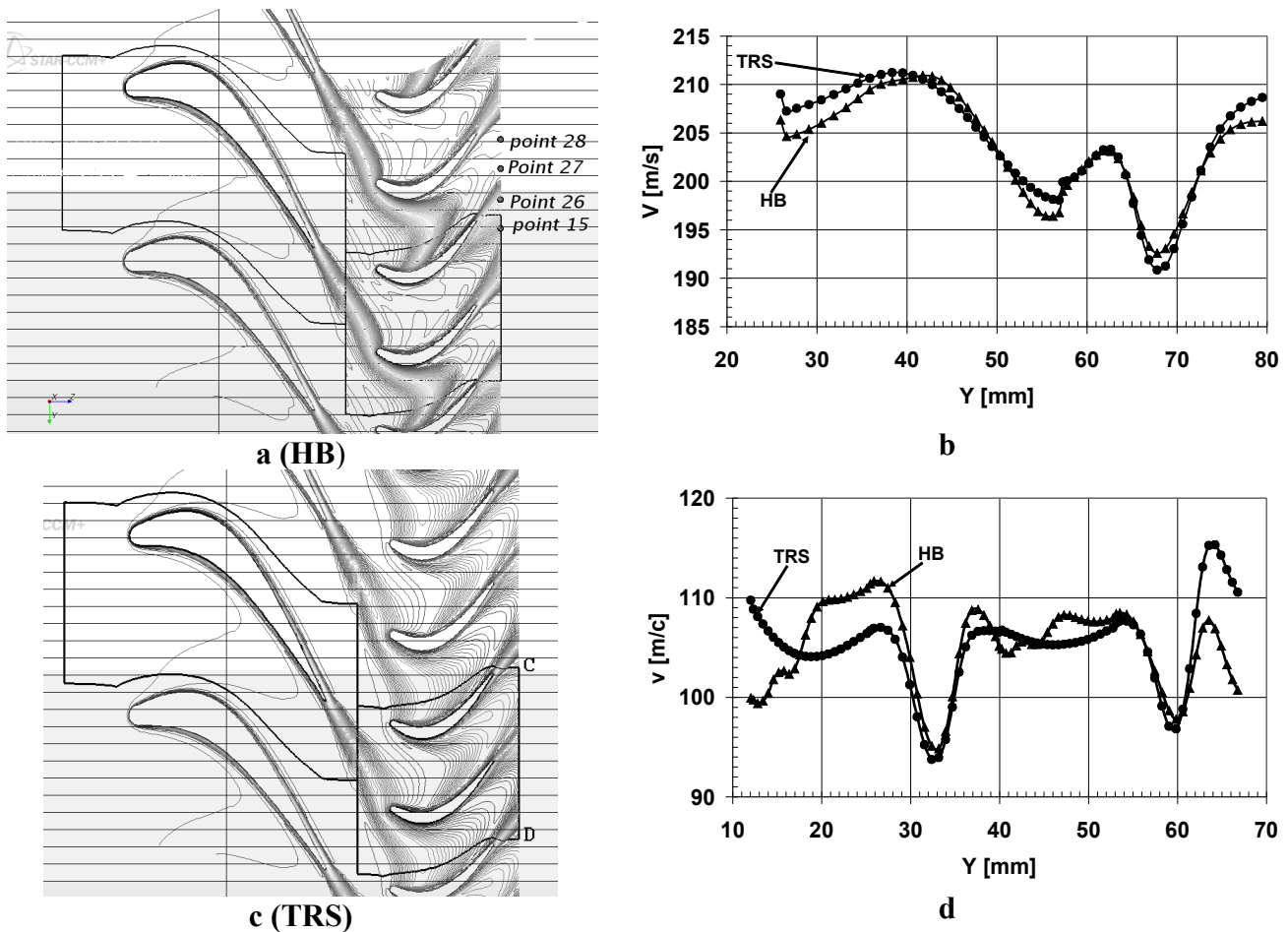


**Figure 6 - Instantaneous predictions of turbulent viscosity at mid-span turbine for the HB and TRS solutions (a), (c); velocity profile on interface line between two rows(b); velocity distribution on exit of the two rotating channels (d).**

Figures 7a, b, c, d display the time averaged and first mode unsteady pressure calculated using the harmonic balance method. Calculation results show good agreement with experimental data (Kondratiev, 1977) for time averaged surface pressure (0 - mode) on the stator (figure.7a). Figure 7b show that role of mode number is small for 0 - mode surface pressure on the rotor.

Figures 7c,d display that three modes is sufficient to accurately capture the first mode unsteady pressure for the single stage with  $St_2 = 0.772$ . Also it is important to notice that surface pressure pulsations can be equal eight percents relatively to mean pressure on leading edge of the rotor

Comparison of calculating results for TRS and HB approaches represents on Figure 8. It is showed that the difference between two methods for time instances of velocity magnitude depend on monitor point place.

Harmonic balance method in selected parameters of the numerical algorithm can generate substantial deviation (Fig. 8a). In the centre of the rotor wake (point №15, Figure 1) the difference between two methods is more than 5%. Apparently, this is due to the fact that point №15 is located in the area of high turbulence (Figure 3, the first column) and is a natural extension of vane wake.

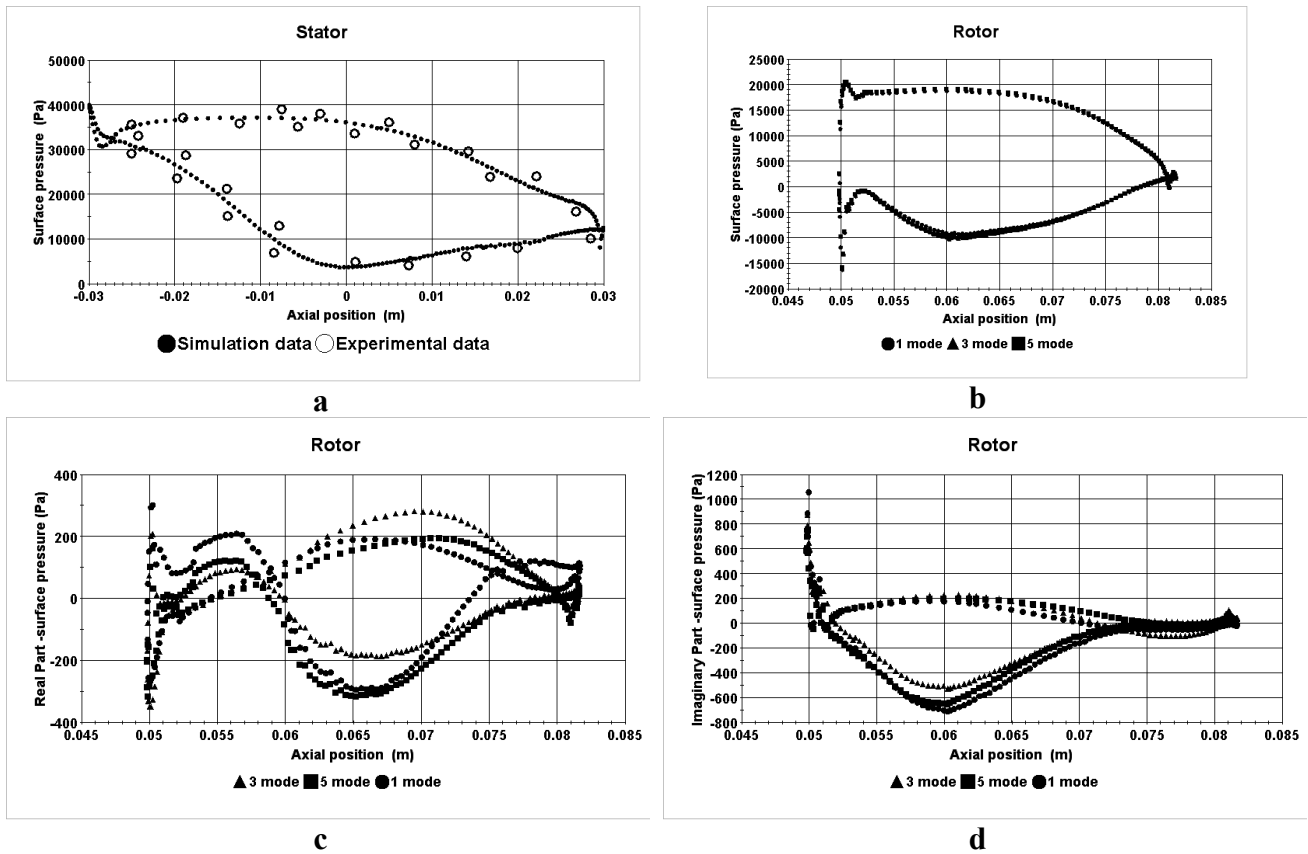


**Figure 7 – Fourier mode 0 on the stator (a); fourier mode 0 on the rotor (b); real part of fourier mode 1 on the rotor (c); imaginary part of fourier mode 1 on the rotor (d).**

At the same time, there has been a satisfactory correspondence between the two approaches to point №27 (Fig. 8b), which is located in the area of low turbulence (Fig. 3, third column).

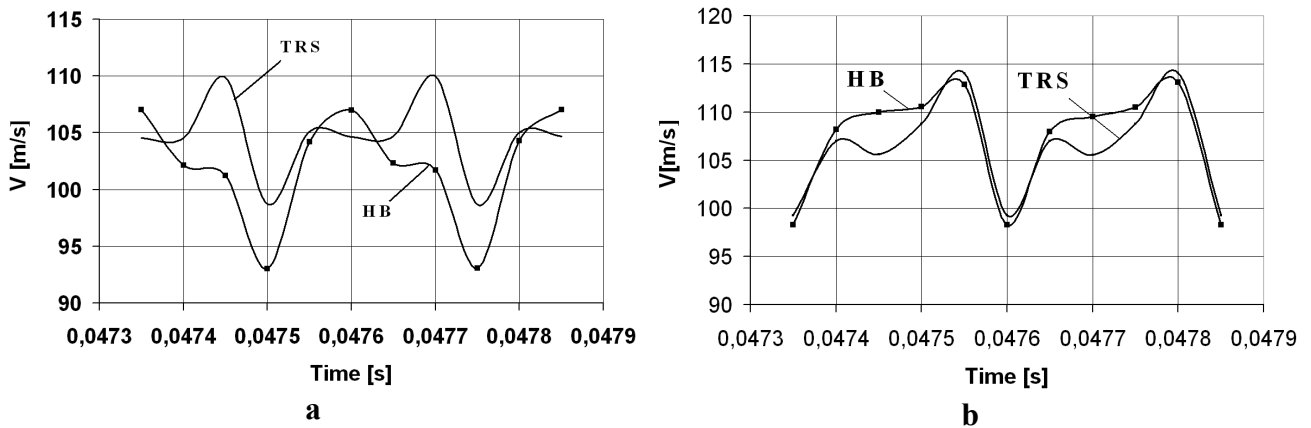


**Figure 8 – Comparison of calculating results for TRS and HB approaches: point 15 on fig. 1 (a); point 27 on fig. 1 (b).**

The results are compared with experimental data on the instantaneous velocity on Figures 9a,b which suggests that both methods (TSR and HB) allow to obtain a satisfactory agreement for the regular (periodic) component of non - stationarity.

A detailed comparison of calculation results with experimental data (Kondratiev V.F., 1977) confirms their satisfactory compliance in the field of low turbulence (point №28, Figure 1). At the same time, there is a noticeable difference, amounting to 10%, in the field of the wake, and the zone adjacent to pressure side of blade where the difference reaches 4% (Fig. 9b).

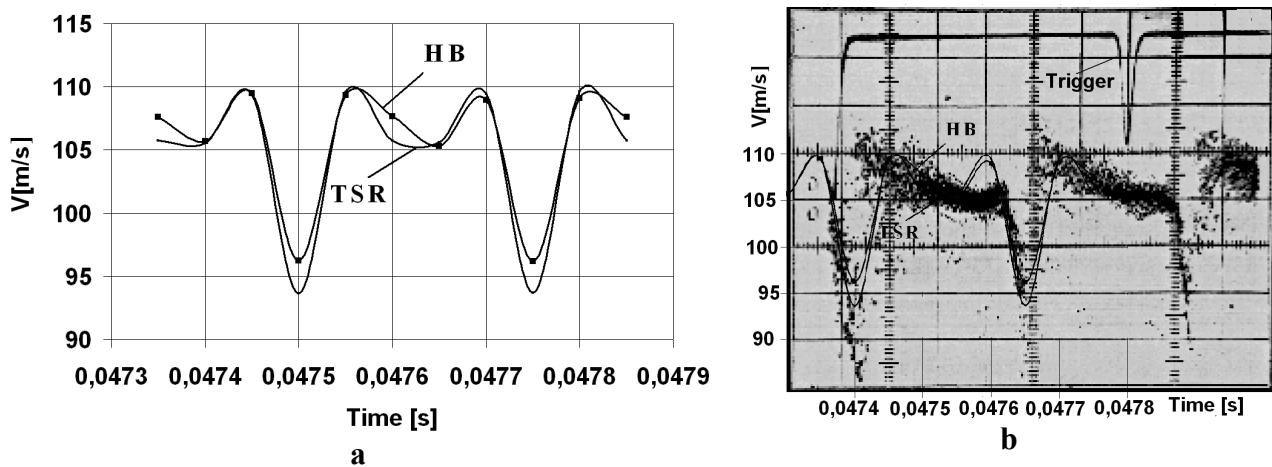


**Figure 9 – Time instances of velocity magnitude 10.2 mm downstream of the rotor trailing edge (a-simulation; b – experimental data for position №28 on fig. 1)**

## CONCLUSIONS

An implicitly coupled nonlinear harmonic balance method implemented within STAR-CCM+ has been used to investigate unsteady flow features of the single stage LPI turbine. The simulation unsteadiness induced by interactions between stator/rotor rows can be performed by means of the harmonic balance method. For stage turbine carried out an accurate comparison of the harmonic (HB) results with those obtained by a sliding-grid simulation (TSR). The ratio of the CPU time required to obtain a periodic solution using the TRS method to the CPU time of the decision on the HB method is 1:2 - five modes, 1:1 - three modes and 3:1 - one mode. Hence, the substantial savings (three times) is observed only in the case of one - mode approximation. It is important to note that in all cases the calculations were carried out at the same calculation grid, including two blades.

It is shown that three modes is sufficient to accurately capture the first mode unsteady pressure for the single stage with the Strouhal number  $St_2 = 0.772$ , exit Reynolds number  $Re_2 = 3.7 \cdot 10^5$ , exit Max number  $M_2 = 0.464$ . A detailed comparison of calculation results with experimental data confirms their satisfactory compliance in the field of low turbulence. At the same time, there is a noticeable difference, amounting to 10%, in the field of the wake, and the zone adjacent to pressure side of blade where the difference reaches 4%.

## REFERENCES

**Breugelmans F.** Resent research in the VKI turbomachinery and propulsion department. [2005] II International Scientific and Technical Conference “Aero Engines of XXI Century”, Moscow. Abstract collection, Vol. I. pp. 16 - 25.

**Biesinger T., Cornelius Ch., Rube C., Schmid G., Braune A., Campregher R., Godin Ph.G., Zori L.** [2010] Unsteady CFD methods in commercial solver for turbomachinery applications. Proceedings of ASME Turbo Expo - 2010: Power for Land, Sea and Air, Glasgow, UK. 12pp.

**Connell S., Braaten M., Zori L., Steed R., Hutchinson B., Cox G.** [2011] A comparison of advanced numerical techniques to model transient flow in turbomachinery blade rows. Proceedings of ASME Turbo Expo - 2011. Vancouver. British Columbia. Canada. 10pp.

**He L., Ning W.** [1998] Efficient approach for analysis of unsteady viscous flows in turbomachines. AIAA J., Vol. 36, No. 11, pp. 2005 - 2012.

**He L., Chen T., Wells R.G., Li Y.S., Ning W.** [2006] Analysis of rotor – rotor and stator – stator interferences in multi – stage turbomachines. Proceedings of GT2006 ASME Turbo Expo - 2006: Power for Land, Sea and Air. Barcelona. Spain. 11pp.

**Hall K.C., Thomas J.P., Clark W.S.** [2002] Computation of unsteady nonlinear flows in cascades using a harmonic balance technique. AIAA J., Vol. 40, No. 5, pp. 879-886.

**Vilmin S., Lorrain E., Hirsch Ch., Swoboda M.** [2009] Unsteady flow modeling across the rotor/stator interface using the nonlinear harmonic method. Proceedings of ASME Turbo - Expo 2009: Power for Land, Sea and Air. Orlando, Florida, USA. 9pp.

**Weiss J.M., Subramanian V., Hall K.C.** [2011] Simulation of unsteady turbomachinery flows using of implicitly coupled nonlinear harmonic balance method. Proceedings of ASME. Turbo Expo – 2011, Vancouver, Canada. 8pp.

**Custer C.H., Weiss J.M., Subramanian V., Clark W. S., Hall K.C.** [2012] Unsteady simulation of a 1.5 stage turbine using an implicitly coupled nonlinear harmonic balance method. Proceedings of ASME Turbo Expo - 2012. Copenhagen. Denmark. 15pp.

**Kondratiev V. F.** [1977] Investigation physical phenomena and unsteady interactions in the turbine stage. PhD thesis. Leningrad, LPI. 206pp. (in Russian).